SPECKLE PHENOMENA IN OPTICS
THEORY AND APPLICATIONS
Second Edition

Joseph W. Goodman

SPIE PRESS
Bellingham, Washington USA

Library of Congress Cataloging-in-Publication Data

Names: Goodman, Joseph W., author.
Title: Speckle phenomena in optics : theory and applications / Joseph W. Goodman.
Identifiers: LCCN 2019033832 (print) | LCCN 2019033833 (ebook) | ISBN 9781510631489 (paperback) | ISBN 9781510631496 (pdf)
Subjects: LCSH: Speckle. | Optics. | Reflection (Optics) | Light–Scattering.
Classification: LCC QC427.8.S64 G66 2020 (print) | LCC QC427.8.S64 (ebook) | DDC 535/.32–dc23
LC record available at https://lccn.loc.gov/2019033832
LC ebook record available at https://lccn.loc.gov/2019033833

Published by

SPIE
P.O. Box 10
Bellingham, Washington 98227-0010 USA
Phone: +1 360.676.3290
Fax: +1 360.647.1445
Email: books@spie.org
Web: http://spie.org

Printed in the United States of America.
First Printing.
For updates to this book, visit http://spie.org and type "PM312" in the search field.

Contents

Preface – Second Edition

To explain the origins of this second edition of *Speckle Phenomena in Optics*, it is first helpful to trace the history of the first edition. The book was originally published by Roberts & Company Publishers (a small startup publisher) in 2007. Roberts & Company was subsequently acquired by MacMillan Publishing Company. The book continued to be published by MacMillan under the Roberts & Company label. In 2019, MacMillan decided not to continue marketing and selling the book, and returned the copyright to me, the author. In the meantime, over a period of three or four years, I had been adding material to the manuscript and making certain revisions to the original manuscript in preparation for an improved second edition. In this Preface, I outline some of the improvements that the reader will find in the second edition.

The first set of improvements I would call "stylistic." A reviewer of the first edition pointed out that some equations (especially those with exponents) had been set in a typeface that was too small to read without a magnifying glass. All equations with this problem have been modified to improve their readability. A second stylistic problem was that in many figures, the curves representing results of the analyses had been drawn with a point size that was too small, so that they appeared too faint in the figures, at least too faint for my taste. This error has been corrected throughout.

In addition to these stylistic changes, considerable material has been added to this new edition:

- A new Section 3.2.4 considers a random walk with random-length phasors, introducing different models for the length statistics;
- A new Section 3.2.5 considers a random walk with a random number of random-length phasors;
- Sections 4.1 through 4.3 have been generalized so that they can be applied to the subject of polarization speckle in later sections;
- In Chapter 4, entirely new Sections 4.5 and 4.6 have been added covering the subject of polarization in speckle patterns, including statistics of the Stokes parameters and polarization speckle;
- Sections 5.5, 5.6, and 5.7 are new simplified explanations of the effects of a change of angle-of-illumination and change of wavelength on the spatial structure of speckle;

- Sections 5.8 and 5.9 are new simplified explanations of the spatial structure of speckle in an in-focus imaging system and an out-of-focus imaging system;
- Section 6.1 in the original edition contained an incorrect discussion of speckle in the eye; this discussion has been corrected in the second edition;
- Section 7.6 is an entirely new discussion of the characteristics of speckle produced by "smooth" surfaces;
- Section 8.3 is a new section discussing how to create a spectrometer that measures the spectrum of a source from the speckle it produces; and
- A number of new references have been introduced in the second edition.

The reader may note that some of the material presented in Chapter 4 of the first edition has been moved to a new Chapter 5 entitled "Spatial Structure of Speckle" in the second edition, a move that seemed logical when coupled with the several new sections introduced in that chapter.

I would like to thank Prof. Mitsuo Takeda and Prof. Wei Wang for educating me on the subject of polarization speckle. I would like to extend a heartfelt thanks to two anonymous reviewers whose comments were extremely helpful in preparing the final version of the manuscript. Again I thank my wife, Hon Mai, for tolerating my many hours at the computer working on this new edition. Finally, I thank Ms. Dara Burrows of SPIE for her extremely careful copy editing of the manuscript; her suggestions improved the book significantly.

Joseph W. Goodman
November 2019

Preface – First Edition

Writing this book was a labor of love! In 1963, after finishing my Ph.D. research in the field of radar countermeasures, the first subject in optics that I studied in detail was speckle. So I began my career in optics with speckle, and it has been gratifying to return to this subject again after more than 40 years.

This book is directed towards a sophisticated audience with a good grasp of Fourier analysis, and a previous exposure to the broad concepts of statistics and random processes. It is suitable for a graduate textbook or a professional reference book. After the introductory chapter, the next three chapters deal with the theory of speckle, while the last last five chapters deal with what I consider to be application areas.

The field of speckle is a broad one, as evidenced by the breadth of the subjects covered here. Inevitably I have failed to reference all those who deserve credit for contributing to this field, and to those I have omitted, I offer my apologies.

This book has been several years in the making, partially because in mid course I was diverted to writing a third edition of *Introduction to Fourier Optics*. I have learned a lot that I didn't know about speckle in the process, and I have many people to thank for this education. To begin, I owe a tremendous debt to Pierre Chavel, of the Institut d'Optique, for reading the entire book and making suggestions and corrections that improved the work immensely. I thank Ben Roberts, of Roberts & Company Publishers, for having faith that a book on this subject would be appropriate for his small publishing company. I also thank Sam Ma, who also did yeoman's duty seeking out misprints and errors. I thank Lee Young, the copy editor who kept my writing clear, consistent, and in good English.

On a finer-grain level, I thank the following for their help with the material in various chapters:

Chapter 4 Kevin Webb, Isaak Freund and Mark Dennis;
Chapter 6 Kevin Webb, James Bliss, Daniel Malacara, Jahja Trisnadi, Michael Morris, Raymond Kostuk, Marc Levinson, and Christer Rydberg;
Chapter 7 Moshe Nazarathy and Amos Agmon;
Chapter 8 Mitsuo Takeda and James Wyant;

Chapter 9 Michael Roggemann and James Fienup; and
Appendix A Rodney Edwards.

All of these individuals helped improve the book. Of course, responsibility for errors rests with me.

Finally, I want to thank my wife, Hon Mai, who did not complain about the many hours I spent writing this book, and in fact encouraged me to push forward on many occasions.

Chapter 1
Origins and Manifestations of Speckle

1.1 General Background

In the early 1960s, when continuous-wave lasers first became commercially available, researchers working with these instruments noticed what at the time was regarded as a strange phenomenon. When laser light was reflected from a surface such as paper, or the wall of the laboratory, a high-contrast, fine-scale granular pattern would be seen by an observer looking at the scattering spot. In addition, measurement of the intensity reflected from such a spot showed that such fine-scale fluctuations of the intensity exist in space, even though the illumination of the spot was relatively uniform. This type of granularity became known as "speckle."

The origin of these fluctuations was soon recognized to be the "random" roughness of the surfaces from which the light was reflected [153], [138].[1] In fact, most materials encountered in the real world are rough on the scale of an optical wavelength (notable exceptions being mirrors). Various microscopic facets of the rough scattering surface contribute randomly phased elementary contributions to the total observed field, and those contributions interfere with one another to produce a resultant intensity (the squared magnitude of the field) that may be weak or strong, depending on the particular set of random phases that may be present.

Speckle is also observed when laser light is transmitted through stationary diffusers, for the same basic reason: the optical paths of different light rays passing through the transmissive object vary significantly in length on the scale of a wavelength. Similar effects are observed when light is scattered from particle suspensions. The speckle phenomenon thus appears frequently in optics; it is in fact the rule rather than the exception. Figure 1.1 shows three photos, the first of a rough object illuminated with incoherent light, the second of the same object illuminated with light from a laser, and the third a

[1]This author also became involved in the study of speckle at about this same time and published a technical report on the subject. See [76].

If in addition the carrier frequency term is suppressed, we have a representation of the form

$$\mathbf{A}(x,\, y;\, t) = A(x,\, y;\, t)\, e^{j\theta(x,y;t)}. \tag{1.3}$$

Note that the real part of $\mathbf{A}(x, y; t)\, e^{-j2\pi\nu_o t}$ is the original real-valued signal we started with.

Such complex representations will be widely used throughout this book. The speckle phenomenon occurs when a resultant complex representation is composed of a superposition (sum) of a multitude of randomly phased "elementary" complex components. Thus, at a single point in space–time,

$$\mathbf{A} = Ae^{j\theta} = \sum_{n=1}^{N} \mathbf{a}_n = \sum_{n=1}^{N} a_n\, e^{j\phi_n}, \tag{1.4}$$

where $\mathbf{a}_n$ is the nth complex phasor component of the sum, having length a_n and phase ϕ_n.

In some cases it is convenient to explicitly represent the time or space dependence of the underlying phasors and/or the resultant. In such cases we might write

$$\mathbf{A}(x,\, y;\, t) = \sum_{n=1}^{N} a_n(x,\, y;\, t) e^{j\phi_n(x,\, y;\, t)}. \tag{1.5}$$

Finally, there may be cases for which the basic phasor components arise from a set of randomly phased complex orthogonal functions, such as modes in a waveguide, in which case the sum may take the form

$$\mathbf{A}(x,\, y;\, t) = \sum_{n=1}^{N} \psi_n(x,\, y;\, t) e^{j\phi_n}. \tag{1.6}$$

With this background, we now turn to a detailed study of the statistics of the length and phase of the resultant phasor under a variety of conditions.

Chapter 2
Random Phasor Sums

In this chapter we examine the first-order statistical properties of the amplitude and phase of various kinds of random phasor sums. By "first-order" we mean the statistical properties at a point in space or, for time-varying speckle, in space–time. While in optics it is generally the *intensity* of the wave that is ultimately of interest, in both ultrasound and microwave imaging, the amplitude[1] and phase of the field can be detected directly. For this reason, we focus attention in this chapter on the properties of the amplitude and phase of the resultant of a random phasor sum. In the chapter that follows, we examine the corresponding properties of the intensity, as appropriate for speckle in the optical region of the spectrum.

A random phasor sum may be described mathematically as follows:

$$\mathbf{A} = Ae^{j\theta} = \frac{1}{\sqrt{N}} \sum_{n=1}^{N} \mathbf{a}_n = \frac{1}{\sqrt{N}} \sum_{n=1}^{N} a_n e^{j\phi_n}, \tag{2.1}$$

where N represents the number of phasor components in the random walk, bold-faced $\mathbf{A}$ represents the resultant phasor (a complex number), italic A represents the length (or magnitude) of the complex resultant, θ represents the phase of the resultant, $\mathbf{a}_n$ represents the nth component phasor in the sum (a complex number), a_n is the length of $\mathbf{a}_n$, and ϕ_n is the phase of $\mathbf{a}_n$. The scaling factor $1/\sqrt{N}$ is introduced here and in what follows in order to preserve finite second moments of the sum even when the number of component phasors approaches infinity.

Throughout our discussions of random walks, it will be convenient to adopt certain assumptions about the statistics of the component phasors that make up the sum. These assumptions are most easily understood by considering the real and imaginary parts of the resultant phasor,

[1]The term "amplitude" will often be used to refer to the modulus of the complex amplitude.

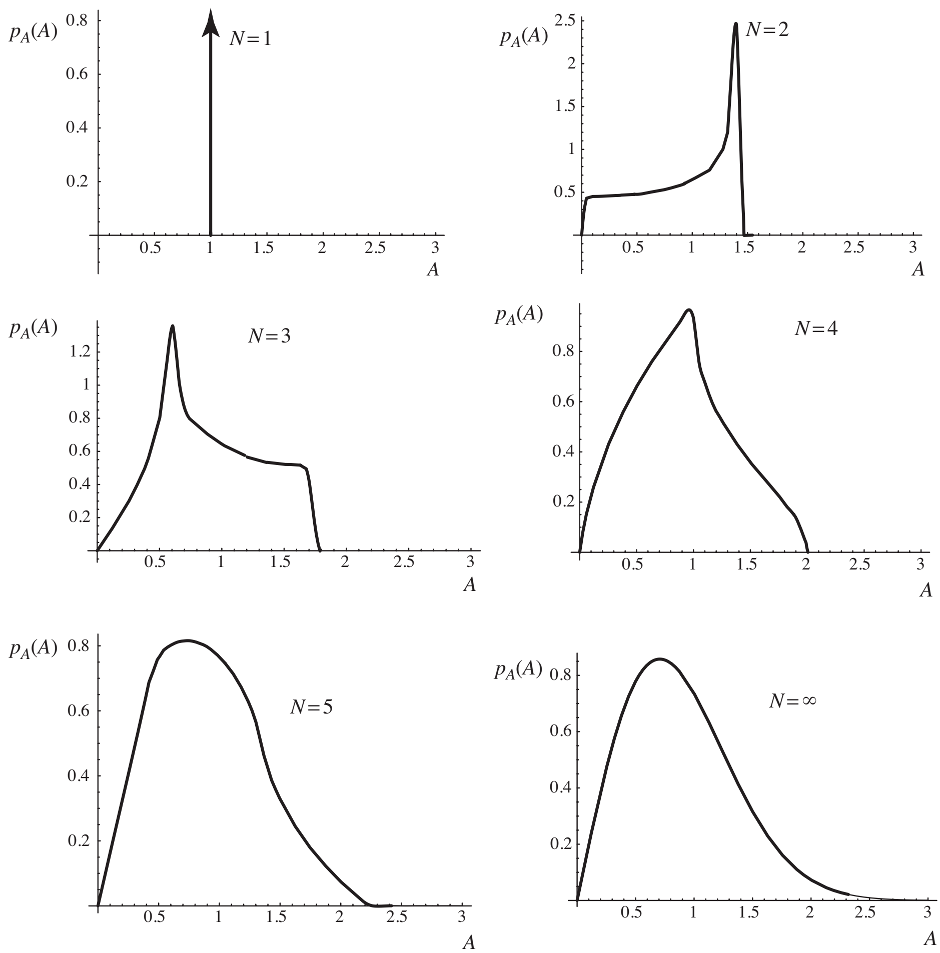

Figure 2.7 Probability density functions of the length A of random phasor sums having N phasors, each with length $1/\sqrt{N}$.

2.6 Random Phasor Sums with a Nonuniform Distribution of Phases

Next we consider a random phasor sum for which the underlying phasor components have a *nonuniform* distribution of phase. We retain the assumption that all components are identically distributed, as well as all assumptions about the independence of the components and independence of the amplitude and phase of any one component.

We begin with the usual equations for the real and imaginary parts of the resultant phasor,

$$
\begin{aligned}
\mathcal{R} &= \frac{1}{\sqrt{N}} \sum_{n=1}^{N} a_n \cos\phi_n \\
\mathcal{I} &= \frac{1}{\sqrt{N}} \sum_{n=1}^{N} a_n \sin\phi_n.
\end{aligned}
\tag{2.42}
$$

$$
\begin{aligned}
\sigma_{\mathcal{R}}^2 &= \frac{\overline{a^2}}{4}[2 + \mathbf{M}_\phi(2) + \mathbf{M}_\phi(-2)] \\
&\quad - \frac{\overline{a}^2}{4}[2\mathbf{M}_\phi(1)\mathbf{M}_\phi(-1) + \mathbf{M}_\phi{}^2(1) + \mathbf{M}_\phi{}^2(-1)] \\
\sigma_{\mathcal{I}}^2 &= \frac{\overline{a^2}}{4}[2 - \mathbf{M}_\phi(2) - \mathbf{M}_\phi(-2)] \\
&\quad - \frac{\overline{a}^2}{4}[2\mathbf{M}_\phi(1)\mathbf{M}_\phi(-1) - \mathbf{M}_\phi{}^2(1) - \mathbf{M}_\phi{}^2(-1)] \\
C_{\mathcal{R},\mathcal{I}} &= \frac{\overline{a^2}}{4j}[\mathbf{M}_\phi(2) - \mathbf{M}_\phi(-2)] - \frac{\overline{a}^2}{4j}[\mathbf{M}_\phi{}^2(1) - \mathbf{M}_\phi{}^2(-1)],
\end{aligned}
\tag{2.47}
$$

where $C_{\mathcal{R},\mathcal{I}}$ signifies the *covariance* of $\mathcal{R}$ and $\mathcal{I}$,

$$
C_{\mathcal{R},\mathcal{I}} = \overline{(\mathcal{R} - \overline{\mathcal{R}})(\mathcal{I} - \overline{\mathcal{I}})}. \tag{2.48}
$$

As a special case, consider phases ϕ_n that obey zero-mean Gaussian statistics. The density function and characteristic function of the phase in this case are

$$
\begin{aligned}
p_\phi(\phi) &= \frac{1}{\sqrt{2\pi}\sigma_\phi} \exp\left(-\frac{\phi^2}{2\sigma_\phi^2}\right) \\
\mathbf{M}_\phi(\omega) &= \exp\left(-\frac{\sigma_\phi^2\,\omega^2}{2}\right).
\end{aligned}
\tag{2.49}
$$

Substitution in Eq. (2.47) yields

$$
\begin{aligned}
\overline{\mathcal{R}} &= \sqrt{N}\overline{a}\, e^{-\sigma_\phi^2/2} \\
\overline{\mathcal{I}} &= 0 \\
\sigma_{\mathcal{R}}^2 &= \frac{\overline{a^2}}{2}\left[1 + e^{-2\sigma_\phi^2}\right] - \overline{a}^2 e^{-\sigma_\phi^2} \\
\sigma_{\mathcal{I}}^2 &= \frac{\overline{a^2}}{2}\left[1 - e^{-2\sigma_\phi^2}\right] \\
C_{\mathcal{R},\mathcal{I}} &= 0.
\end{aligned}
\tag{2.50}
$$

As an aside we note that both $\overline{\mathcal{I}}$ and $C_{\mathcal{R},\mathcal{I}}$ will always vanish for any *even* probability density function for the ϕ_n.

Figure 2.8 shows a contour plot of the (approximate) joint density function of $\mathcal{R}$ and $\mathcal{I}$ when $N = 100$ and $\sigma_\phi = 1$ rad. In this plot we have assumed that all component phasors have length 1. Note that the contours are

Chapter 4
Higher-Order Statistical Properties of Speckle

Based on the material presented in Chapter 3, the statistical properties of optical speckle at a single point in space (or, for dynamically changing speckle, a single point in time) are understood. Now we turn to the joint properties of two or more speckles, which can represent samples of a single statistically stationary speckle pattern, or, in the bivariate case, the statistics of two polarization components of a speckle pattern at a single point in space or time.

4.1 Multivariate Gaussian Statistics

The underlying statistical model for a fully developed speckle field is that of a circular complex Gaussian random process, with real and imaginary parts that are real-valued, jointly Gaussian random processes. It is therefore necessary to begin with a brief discussion of multivariate Gaussian distributions.

The characteristic function of an M-dimensional set of real-valued Gaussian random variables represented by a column vector $\vec{u} = \{u_1, u_2, \ldots, u_M\}^t$ is given by

$$\mathbf{M}_u(\vec{\omega}) = \exp\left\{j\vec{\bar{u}}^t\vec{\omega} - \frac{1}{2}\vec{\omega}^t\underline{\mathcal{C}}\,\vec{\omega}\right\}, \tag{4.1}$$

where a superscript t indicates a matrix transpose, $\vec{\bar{u}}$ is a column vector of the means of the u_m, and $\vec{\omega}$ is a column vector with components $\omega_1, \omega_2, \ldots, \omega_M$. The symbol $\underline{\mathcal{C}}$ represents the covariance matrix, that is, a matrix with element $c_{n,m}$ at the intersection of the nth row and the mth column, given by following expected value:

$$c_{n,m} = E[(u_n - \overline{u_n})(u_m - \overline{u_m})]. \tag{4.2}$$

$$\vec{u} = \{\mathcal{R}_1, \mathcal{R}_2, \ldots, \mathcal{R}_N, \mathcal{I}_1, \mathcal{I}_2, \ldots, \mathcal{I}_N\}^t.$$

Because the fields of interest are *circular* complex random variables $\mathbf{A}_n$ and $\mathbf{A}_m$, we have

$$\begin{aligned}
\overline{\mathcal{R}_n} = \overline{\mathcal{I}_n} = \overline{\mathcal{R}_m} &= \overline{\mathcal{I}_m} = 0 \\
\overline{\mathcal{R}_n^2} &= \overline{\mathcal{I}_n^2} = \sigma_n^2 \\
\overline{\mathcal{R}_m^2} &= \overline{\mathcal{I}_m^2} = \sigma_m^2 \\
\overline{\mathcal{R}_n\mathcal{I}_n} &= \overline{\mathcal{R}_m\mathcal{I}_m} = 0 \\
\overline{\mathcal{R}_n\mathcal{I}_m} &= -\overline{\mathcal{R}_m\mathcal{I}_n} \\
\overline{\mathcal{R}_n\mathcal{R}_m} &= \overline{\mathcal{I}_n\mathcal{I}_m}.
\end{aligned} \tag{4.7}$$

The form of the probability density function in Eq. (4.3) becomes

$$p(\vec{u}) = \frac{1}{(2\pi)^N |\underline{\mathcal{C}}|^{1/2}} \exp\left[-\frac{1}{2}\vec{u}^t \underline{\mathcal{C}}^{-1} \vec{u}\right], \tag{4.8}$$

where

$$\underline{\mathcal{C}} = \begin{bmatrix} \overline{\mathcal{R}_1\mathcal{R}_1} & \overline{\mathcal{R}_1\mathcal{R}_2} & \cdots & \overline{\mathcal{R}_1\mathcal{I}_N} \\ \overline{\mathcal{R}_2\mathcal{R}_1} & \overline{\mathcal{R}_2\mathcal{R}_2} & \cdots & \overline{\mathcal{R}_2\mathcal{I}_N} \\ & & \vdots & \\ \overline{\mathcal{I}_1\mathcal{R}_1} & \overline{\mathcal{I}_1\mathcal{R}_2} & \cdots & \overline{\mathcal{I}_1\mathcal{I}_N} \\ & & \vdots & \\ \overline{\mathcal{I}_N\mathcal{R}_1} & \overline{\mathcal{I}_N\mathcal{R}_2} & \cdots & \overline{\mathcal{I}_N\mathcal{I}_N} \end{bmatrix}. \tag{4.9}$$

The relations of Eq. (4.7) can then be used to simplify this matrix.

A general result derived from Eq. (4.5) and the properties described above holds for joint moments of circular complex Gaussian random variables $\mathbf{A}_1, \mathbf{A}_2, \ldots, \mathbf{A}_{2k}$:

$$\overline{\mathbf{A}_1^*\mathbf{A}_2^* \cdots \mathbf{A}_k^*\mathbf{A}_{k+1}\mathbf{A}_{k+2} \cdots \mathbf{A}_{2k}} = \sum_{\Pi} \overline{\mathbf{A}_1^*\mathbf{A}_p}\,\overline{\mathbf{A}_2^*\mathbf{A}_q} \cdots \overline{\mathbf{A}_k^*\mathbf{A}_r}, \tag{4.10}$$

where $\sum_\Pi$ represents a summation over the $k!$ possible permutations $(p, \ldots, r)$ of $(1, 2, \ldots, k)$. This result will be called the *complex Gaussian moment theorem*. For the special case of four of such variables ($k = 2$), we have

$$\overline{\mathbf{A}_1^*\mathbf{A}_2^*\mathbf{A}_3\mathbf{A}_4} = \overline{\mathbf{A}_1^*\mathbf{A}_3}\,\overline{\mathbf{A}_2^*\mathbf{A}_4} + \overline{\mathbf{A}_1^*\mathbf{A}_4}\,\overline{\mathbf{A}_2^*\mathbf{A}_3}. \tag{4.11}$$

and $\mathbf{A}_2$. The problem remains to integrate Eq. (4.21) to find the marginal density functions of interest.

4.3.2 Joint density function of the amplitudes

To find the joint density function of the amplitudes A_1 and A_2, we integrate Eq. (4.21) with respect to θ_1 and θ_2. To simplify the integration, first hold θ_2 constant and consider the integration with respect to θ_1. Because we are integrating over one full period of the cos function, we can as well integrate a new variable $\alpha = \phi + \theta_1 - \theta_2$ over a full period of 2π rad. Thus the integral becomes

$$\begin{aligned} p(A_1, A_2) = {} & \int_{-\pi}^{\pi} d\theta_2 \int_{-\pi}^{\pi} d\alpha \frac{A_1 A_2}{4\pi^2 \sigma_1^2 \sigma_2^2 (1-\mu^2)} \\ & \times \exp\left[-\frac{\sigma_2^2 A_1^2 + \sigma_1^2 A_2^2 - 2 A_1 A_2 \sigma_1 \sigma_2 \mu \cos(\alpha)}{2\sigma_1^2 \sigma_2^2 (1-\mu^2)} \right]. \end{aligned} \tag{4.22}$$

The integrals are readily performed, with the result

$$p(A_1, A_2) = \frac{A_1 A_2}{\sigma_1^2 \sigma_2^2 (1-\mu^2)} \exp\left(-\frac{\sigma_2^2 A_1^2 + \sigma_1^2 A_2^2}{2\sigma_1^2 \sigma_2^2 (1-\mu^2)} \right) I_0 \left[\frac{\mu A_1 A_2}{\sigma_1 \sigma_2 (1-\mu^2)} \right], \tag{4.23}$$

where I_0 is again a modified Bessel function of the first kind, order zero, and the result is valid for $0 \le A_1, A_2 \le \infty$.

As a check on this result, we find the marginal density function of a single amplitude, A_1,

$$p(A_1) = \int_0^{\infty} p(A_1, A_2)\, dA_2 = \frac{A_1}{\sigma_1^2} \exp\left(-\frac{A_1^2}{2\sigma_1^2} \right), \tag{4.24}$$

which is a *Rayleigh* density, in agreement with previous results.

Figure 4.1 illustrates the shape of the normalized joint density function $\sigma_1 \sigma_2 p(A_1, A_2)$ for various values of μ. The figures on the right are contour plots of the figures on the left. It can be seen that, as the correlation coefficient increases, the joint density function approaches a shaped delta-function sheet along the line $A_1 = A_2$.

Another quantity of interest is the *conditional* density of A_1, given that the value of A_2 is known. This density function is represented by $p(A_1|A_2)$ and can be found using Bayes' rule,

Chapter 7
Speckle in Certain Imaging Applications

7.1 Speckle in the Eye

An interesting experiment can be performed with a group of people in a room using a CW laser (even a small laser pointer will do if the beam is expanded a bit and the lights are dimmed). Shine the light from the laser on the wall or on any other planar rough scattering surface and ask the members of the group to remove any eyeglasses they may be wearing (this may be difficult to do for people with contact lenses, in which case they can continue to wear their lenses). Ask all members of the group to look at the scattering spot and to move their heads laterally left to right and right to left several times. Now ask if the speckles in the spot moved in the same direction as their head movement or in the opposite direction to their head movement. The results will be as following:

- Individuals who have perfect vision or who are wearing their vision correction will report that speckle motion was hard to detect. In effect, the speckle structure appears fixed to the surface of the scattering spot and does not appear to move *with respect to the spot*, but does undergo some internal change that is not motion.
- Individuals who are farsighted and uncorrected will report that the speckle moved in the same direction as their head moved, translating through the scattering spot in that direction.
- Individuals who are nearsighted will report that the speckles move through the scattering spot in the opposite direction to their head movement.

Our goal in this section is to give a brief explanation of the results of this experiment. For alternative but equivalent approaches to explaining this phenomenon, see [11], [128], or [57], page 140.

Let the object consist of an illuminated scattering spot on a planar rough surface, as shown in Fig. 7.1. Let the direction of illumination and the

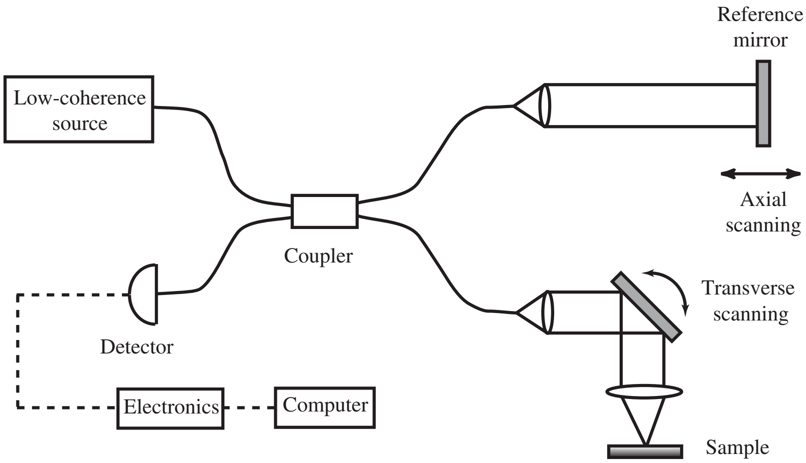

Figure 7.4 A fiber-based interferometer for use in OCT. The axial scanning mirror changes the path-length delay in the reference arm to select the axial depth, and the transverse scanning mirror selects the transverse coordinates being imaged.

where the coherence with respect to a reference beam is high can be distinguished from depth regions where that coherence has vanished. Figure 7.4 illustrates one possible realization of an OCT system. The system is a fiber-based Michelson interferometer. It operates by linearly scanning the reference mirror in the axial direction to scan the region of high coherence through the depth of the object, and scanning the mirror in the object arm to move the region of measurement in the transverse direction across the object. In this fashion a 2D scan of the object is obtained.[2] The linear motion of the reference mirror in effect Doppler shifts the reference light, and when the reference and object beams are incident on the detector, a beat note is observed when the light coming from the object is coherent with the light coming from the reference mirror. Thus the amplitude of scattering from the region of high coherence can be determined by measuring the strength of the beat note. As the reference mirror scans, the scattering amplitudes from the corresponding depth regions within the object are obtained.

7.3.2 Analysis of OCT

To understand the operation of OCT in more detail, we embark on a short analysis. Incident on the detector are a reference wave and an object wave, which we represent by analytic signals $\mathbf{E}_r(t)$ and $\mathbf{E}_o(x, z, t)$, respectively,

[2]Several different modes of scanning are possible. By analogy with ultrasound imaging modes, a single vertical scan in the depth direction is referred to as an "A-scan," while the combination of scanning in depth and one transverse direction is referred to as a "B-scan."

7.5.2 Temporal speckle

The speckle phenomenon of concern here is not the usual speckle caused by reflection of light from a rough surface, but rather the temporal intensity fluctuations associated with light from a source with a coherence time that is much longer than the coherence time of typical incoherent sources. The authors of [160] have referred to this type of speckle as "dynamic" speckle. Here we prefer to use the term "temporal speckle," since "dynamic speckle" has a different meaning in the field of speckle metrology.

As was discussed in some detail on page 262, the temporal fluctuations of intensity of a polarized nonlaser source obey the same statistics in time that conventional speckle obeys over space, namely the intensity obeys a negative-exponential distribution. Therefore it is reasonable to call such fluctuations "temporal speckle." Most of the spatial properties of conventional speckle also hold for the temporal properties of temporal speckle.

The energy to which the photoresist is subjected at any point consists of the integrated light intensity contributed by the multiple pulses used for a single exposure. There is a finite number of coherence times within that train of pulses, and as a consequence there can remain residual fluctuations of intensity associated with the integrated intensity. Consistent with the discussion in the subsection beginning on page 99, for a single laser pulse with intensity pulse shape $P_T(t)$, the number of degrees of freedom M_1 is given by

$$M_1 = \frac{\left(\int_{-\infty}^{\infty} P_T(t)\,dt\right)^2}{\int_{-\infty}^{\infty} K_T(\tau)|\boldsymbol{\mu}_{\mathbf{A}}(\tau)|^2\,d\tau}, \tag{7.76}$$

and the contrast of time-integrated speckle from one pulse is given by

$$C = \frac{\left[\int_{-\infty}^{\infty} K_T(\tau)|\boldsymbol{\mu}_{\mathbf{A}}(\tau)|^2\,d\tau\right]^{1/2}}{\int_{-\infty}^{\infty} P_T(t)\,dt}, \tag{7.77}$$

where $K_T(\tau)$ is the autocorrelation function of $P_T(t)$.

In the present case, we take the spectrum of the laser, normalized to have unity area, to be Gaussian, as in Eq. (7.24),

$$\hat{\mathcal{G}}(\nu) = \frac{2\sqrt{\ln 2}}{\sqrt{\pi}\Delta\nu}\,\exp\left[-\left(2\sqrt{\ln 2}\,\frac{\nu+\bar{\nu}}{\Delta\nu}\right)^2\right], \tag{7.78}$$

where $\Delta\nu$ is again the full width at half maximum (FWHM) of the spectrum. The squared magnitude of the complex coherence factor is

$$|\boldsymbol{\mu}_{\mathbf{A}}(\tau)|^2 = \exp\left[-\frac{\pi^2\Delta\nu^2\tau^2}{2\ln 2}\right]. \tag{7.79}$$

Chapter 9
Speckle and Metrology

One could argue whether speckle metrology is an imaging or a nonimaging application of speckle. On the one hand, most speckle interferometry systems have an imaging system that is used in gathering information. On the other hand, it is not the image of the object that is really of interest; rather it is information about mechanical properties of the object, such as movement, vibration modes, or surface roughness, that is desired. For this reason, plus the fact that speckle metrology is a well-developed field on its own, we have chosen to have a separate chapter devoted to this subject. While speckle has been a nuisance in almost all of the applications we have discussed previously, in the field of metrology, speckle is put to good use. Applications that use speckle for measurements of displacements arose in the late 1960s and early 1970s, often as an alternative to holographic interferometry. A number of survey articles and books cover the subject extremely well, including [47], [57], [45], [100], [167], and [146].

The field of speckle metrology has so many facets and so many applications that it is difficult to do it justice in a single chapter. At best we can only scratch the surface of such a rich and diverse field. We therefore restrict our goals to introducing some of the basic concepts while referring the reader to the more detailed treatments referenced above for a more in-depth study and more complete bibliographies.

9.1 Speckle Photography

The term "speckle photography" refers to a variety of techniques that use superposition of two speckle intensity patterns, one from a rough object in an initial state and a second from the same object after it is subjected to some form of displacement. Particularly important early work on speckle photography includes that of Burch and Tokarski [25], Archibold, Burch and Ennos [4], and Groh [88]. Figure 9.1 shows typical geometries for the measurement. Part (a) of the figure shows the recording geometry. A diffusely reflecting, optically rough surface is illuminated by coherent light. An imaging brings us to the fringe plane. A further Fourier transform of the fringe, followed by a modulus operation, takes us to the final plane, where the autocorrelation function of the specklegram is obtained. Figure 9.3 shows on the left the fringe patterns obtained when the shift between speckle patterns is 16, 32, 64, and 128 pixels. On the right are the corresponding autocorrelation

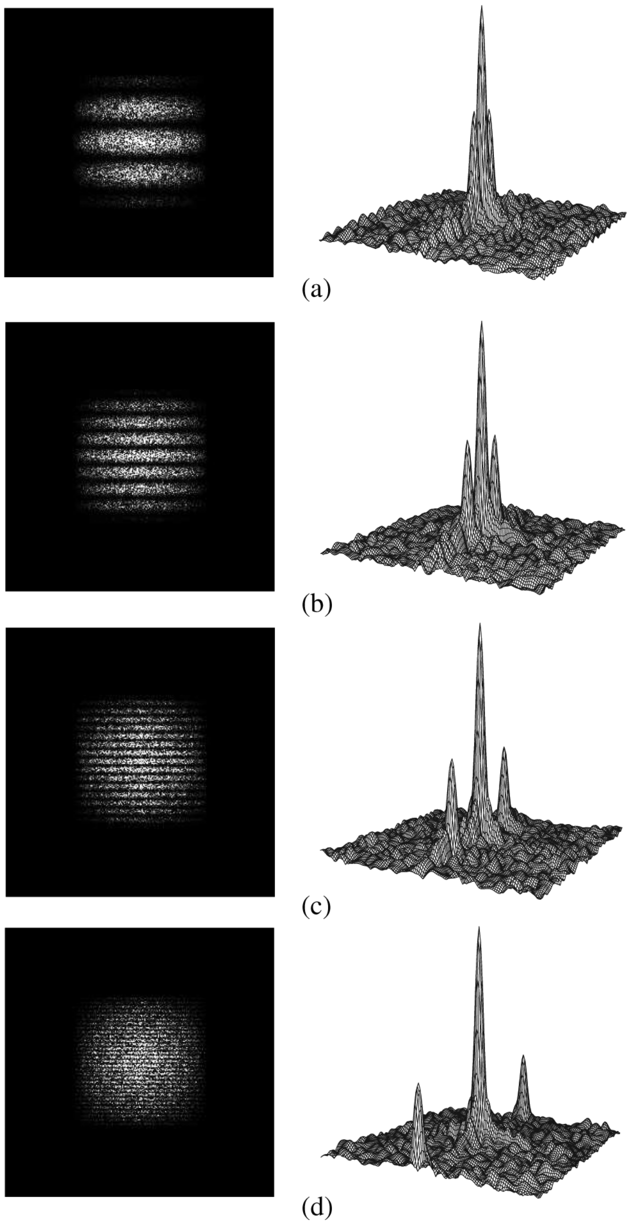

Figure 9.3 Spectral fringe patterns on the left and specklegram autocorrelation functions on the right for object translations of (a) 16 pixels, (b) 32 pixels, (c) 64 pixels, and (d) 128 pixels.

Appendix A
Linear Transformations of Speckle Fields

In this appendix we explore whether a linear transformation of a vector with components consisting of circular complex Gaussian random variables yields a new vector with components that are likewise circular complex Gaussian random variables. Let the original vector be

$$\underline{\mathcal{A}} = \begin{bmatrix} \mathbf{A}_1 \\ \mathbf{A}_2 \\ \vdots \\ \mathbf{A}_N \end{bmatrix}, \tag{A.1}$$

where $\mathbf{A}_1, \mathbf{A}_2, \ldots, \mathbf{A}_N$ are known to be circular complex Gaussian random variables. Consider a new vector $\underline{\mathcal{A}}'$, defined by

$$\underline{\mathcal{A}}' = \underline{\mathcal{L}}\underline{\mathcal{A}}, \tag{A.2}$$

with

$$\underline{\mathcal{A}}' = \begin{bmatrix} \mathbf{A}_1' \\ \mathbf{A}_2' \\ \vdots \\ \mathbf{A}_N' \end{bmatrix} \tag{A.3}$$

and

$$\underline{\mathcal{L}} = \begin{bmatrix} \mathbf{L}_{11} & \mathbf{L}_{12} & \ldots & \mathbf{L}_{1N} \\ \mathbf{L}_{21} & \mathbf{L}_{22} & \ldots & \mathbf{L}_{2N} \\ \vdots & \vdots & & \vdots \\ \mathbf{L}_{N1} & \mathbf{L}_{N2} & \ldots & \mathbf{L}_{NN} \end{bmatrix}. \tag{A.4}$$

The Gaussianity of the elements of the transformed matrix $\underline{\mathcal{A}}'$ is guaranteed by the fact that any *linear* transformation of Gaussian random